### Pinning and transport of cyclotron/Landau orbits by electromagnetic vortices

Iwo Bialynicki-Birula\*

Center for Theoretical Physics, Polish Academy of Sciences,
Al. Lotników 32/46, 02-668 Warsaw, Poland and
Institute of Theoretical Physics, Warsaw University

Tomasz Radożycki<sup>†</sup>
Chair of Mathematical Methods in Physics, Physics Department,
Warsaw University, Hoża 74, 00-682 Warsaw, Poland

Electromagnetic waves with phase defects in the form of vortex lines combined with a constant magnetic field are shown to pin down cyclotron orbits (Landau orbits in the quantum mechanical setting) of charged particles at the location of the vortex. This effect manifests itself in classical theory as a trapping of trajectories and in quantum theory as a Gaussian shape of the localized wave functions. Analytic solutions of the Lorentz equation in the classical case and of the Schrödinger or Dirac equations in the quantum case are exhibited that give precise criteria for the localization of the orbits. There is a range of parameters where the localization is destroyed by the parametric resonance. Pinning of orbits allows for their controlled positioning — they can be transported by the motion of the vortex lines.

#### PACS numbers: 42.50.Vk, 03.65.-w, 45.50.-j, 52.20.Dq

#### I. INTRODUCTION

The transverse motion of charged particles in a constant magnetic field is fully delocalized. The classical trajectories of particles projected on the plane perpendicular to the field are circles which can be moved around without changing the particle energy. The wave functions of a particle in quantum mechanics exhibit the same behavior. If  $\psi(\mathbf{r})$  is a solution of the Schrödinger or the Dirac equation with the energy E, then a shifted wave function  $\exp(ie\mathbf{r}\cdot(\mathbf{r}_0\times\mathbf{B})/2\hbar)\psi(\mathbf{r}-\mathbf{r}_0)$  is also a solution with the same energy. In the present paper we shall show that electromagnetic beams with vortex lines localize the classical and quantum states at the position of the vortex and when the vortex line is moved, the orbits will follow. In order to describe these properties quantitatively we shall use new exact solutions of the equations of motion obtained in the presence of an electromagnetic field comprising a constant magnetic field and a wave with a vortex line. A related problem — the motion of a particle in a constant magnetic field and a plane electromagnetic wave — has been treated in detail by Roberts and Buchsbaum [1] long time ago. The crucial difference between these two cases is that the translational symmetry in the plane perpendicular to the magnetic field is broken by the presence of an electromagnetic vortex and the problem becomes truly three-dimensional. The present paper on the one hand adds a new twist to the results obtained by Roberts and Buchsbaum and on the other hand it extends our earlier analysis [2] by adding a constant magnetic field.

## \*Electronic address: birula@cft.edu.pl †Electronic address: torado@fuw.edu.pl

## II. THE SIMPLEST ELECTROMAGNETIC BEAM WITH A VORTEX LINE

The notion of a vortex line of the electromagnetic field can be traced back to an old paper by Rainich [4]. A detailed analysis with many examples has been recently given by us in [5]. In the present paper we shall use only a very special case of the vortex line — the one that is found in null solutions of the Maxwell equations [6]. In reality, vortex lines of electromagnetic field are most commonly found in beams carrying angular momentum [7]. The best known examples of such beams are the Bessel beams and the exact Laguerre-Gauss beams. These are solutions of the Maxwell equations obtained by separating the variables in cylindrical coordinates [8]. A convenient description of these beams in terms of just one complex function is obtained with the use of a complex vector

$$F(r,t) = E(r,t) + icB(r,t), \tag{1}$$

which we named the Riemann-Silberstein (RS) vector [9]. The RS vector obeys the complex form of Maxwell equations

$$\partial_t \mathbf{F}(\mathbf{r}, t) = -ic\nabla \times \mathbf{F}(\mathbf{r}, t), \quad \nabla \cdot \mathbf{F}(\mathbf{r}, t) = 0.$$
 (2)

We shall use a representation of  ${\bf F}$  in terms of just one complex function

$$F_x = (\partial_x \partial_z + \frac{i}{c} \partial_y \partial_t) \chi, \tag{3a}$$

$$F_y = (\partial_y \partial_z - \frac{i}{c} \partial_x \partial_t) \chi, \tag{3b}$$

$$F_z = -(\partial_x^2 + \partial_y^2)\chi. \tag{3c}$$

where  $\chi$  is an arbitrary complex solution of the wave equation

$$\left(\frac{1}{c^2}\partial_t^2 - \Delta\right)\chi(\boldsymbol{r}, t) = 0. \tag{4}$$

An equivalent representation of the electromagnetic field expressed in terms of two real solutions of the wave equation, instead of a single complex solution of the wave equation, has been given by Whittaker [10]. The functions  $\chi(\mathbf{r},t)$  for the Bessel beams and for the Laguerre-Gauss beams are [11]

$$\chi_B(\rho, \phi, z, t) = e^{-i\sigma(\omega_k t - k_z z - m\phi)} J_m(k_\perp \rho),$$

$$\chi_{LG}(\rho, \phi, z, t) = \frac{e^{-i\sigma(\omega t_- - m\phi)} \rho^m}{a(t_+)^{n+m+1}}$$

$$\times \exp\left(-\frac{\rho^2}{a(t_+)}\right) L_n^m\left(\frac{\rho^2}{a(t_+)}\right),$$
 (5b)

where  $\sigma = \pm 1$ ,  $t_{\pm} = t \pm z/c$ , and  $a(t_{+}) = l^{2} + i\sigma c^{2}t_{+}/\omega$ . The parameter l determines the transverse size (waist) of the LG beam. In the limit, when  $k_{\perp} \to 0$  for Bessel beams and  $l \to \infty$  for LG beams, both functions (5) for m > 0 reduce (apart from numerical prefactors) to the same solution of the wave equation

$$\chi(\mathbf{r},t) = (x+iy)^m e^{-i\sigma\omega(t-z/c)}.$$
 (6)

This choice of  $\chi$  leads to the following RS vector

$$\mathbf{F}(\mathbf{r},t) = \sigma \left(\hat{\mathbf{x}} + i\hat{\mathbf{y}}\right) (x + iy)^{m-1} e^{-i\sigma\omega(t - z/c)}, \qquad (7)$$

where we again disregarded some numerical prefactors. The RS vector (7) is a good approximation to Laguerre-Gauss and Bessel beams near the z axis, when  $\rho \ll l$  or  $\rho k_{\perp} \ll 1$ . It belongs to a family of the solutions of the Maxwell equations describing vortex lines riding atop of a null electromagnetic field [6]. In the present case, this null field is simply a circularly polarized plane wave

$$\mathbf{F}_0(\mathbf{r},t) = (\hat{\mathbf{x}} + i\hat{\mathbf{y}}) e^{-i\sigma\omega(t-z/c)}.$$
 (8)

The simplest solution, the one with a unit vortex strength, is obtained by choosing m=2 in Eq. (7). In this case, the electric and magnetic field vectors are

$$\boldsymbol{E}(\boldsymbol{r},t) = \sigma B\omega \left( f(\boldsymbol{r},t), g(\boldsymbol{r},t), 0 \right), \tag{9a}$$

$$\boldsymbol{B}(\boldsymbol{r},t) = \sigma \frac{B\omega}{c} \left( -g(\boldsymbol{r},t), f(\boldsymbol{r},t), 0 \right), \tag{9b}$$

where we introduced the field amplitude expressed in terms of the magnetic field strength and

$$f(\mathbf{r},t) = x\cos\omega(t - z/c) + \sigma y\sin\omega(t - z/c), \quad (10a)$$

$$q(\mathbf{r}, t) = \sigma x \sin \omega (t - z/c) - y \cos \omega (t - z/c). \tag{10b}$$

The expressions (9) and (10) show that the sign factor  $\sigma$  determines the helicity — the sense of rotation of the pair of vectors E and B. At each point this pair of vectors rotates with the wave frequency  $\omega$  but, in contrast to

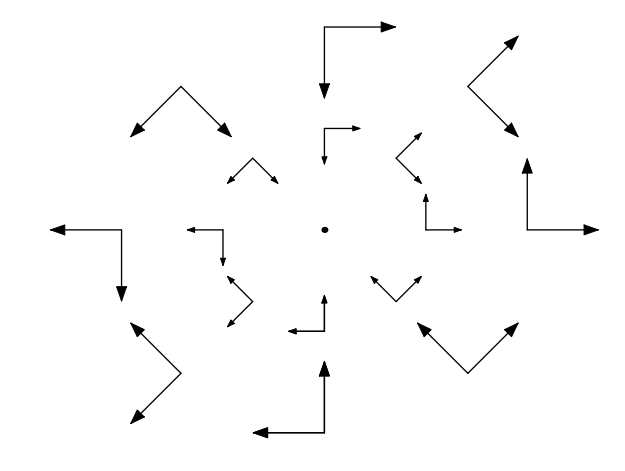


FIG. 1: This figure shows the orientation and the strength of the electric and magnetic field vectors at t=0 and z=0 for the solution of the Maxwell equations with a vortex line described by (9). The point in the middle represents the position of the vortex line. All plots in this paper were generated with the help of Mathematica [3].

the circularly polarized plane wave, the orientation of this pair changes as we move around the vortex line (see Fig. 1). In our case, since the vortex has a unit strength, the total change is  $2\pi$ .

We have shown recently [2] that there exist analytic solutions in the classical and quantum theory describing the motion of charged particles in the presence of the electromagnetic beam (9). Exact solutions exist because the transverse motion (in the plane perpendicular to the direction of the beam propagation) almost separates from the longitudinal motion. The separation is not complete but the longitudinal motion influences only the value of the integration constant appearing in the equations of motion describing the transverse dynamics. The exact solvability is not destroyed by the presence of an additional constant magnetic field aligned with the beam direction. The presence of this field adds a new dimension to the space of control parameters and significantly enriches the dynamical behavior of the system.

The electromagnetic field (9) may seem unrealistic since its amplitude increases without bound with growing distance from the z axis. However, we shall show that the particle is often confined to a region close to the z axis and feels practically the same field as that of much more realistic Laguerre-Gauss or Bessel beams. This expectation has been recently fully confirmed in [12] where we have shown that numerical solutions of the Lorentz equation in the presence of Bessel beams near the vortex line exhibit the same behavior as the analytic solutions found in [2] for the model wave (9).

#### III. CLASSICAL MECHANICS

We shall give first a fully relativistic description of the motion because the nonrelativistic approximation can be easily obtained from the relativistic solution by taking the limit  $c \to \infty$ .

#### A. Relativistic motion

The Lorentz equations of motion

$$m \ddot{\xi}^{\mu}(\tau) = e f^{\mu\nu}(\xi(\tau))\dot{\xi}_{\nu}(\tau), \tag{11}$$

that govern the motion of a relativistic particle moving in the presence of the electromagnetic wave (9) and a constant magnetic field  $\mathbf{B}_0 = (0, 0, B_0)$ , aligned with the beam direction, can be written in the form

$$\ddot{\xi} = \sigma \omega_c \,\omega \, f(\xi, \eta, \zeta, \theta) \left( \dot{\theta} - \dot{\zeta}/c \right) + \omega_0 \dot{\eta}, \tag{12a}$$

$$\ddot{\eta} = \sigma \omega_c \,\omega \,g(\xi, \eta, \zeta, \theta) \left(\dot{\theta} - \dot{\zeta}/c\right) - \omega_0 \dot{\xi},\tag{12b}$$

$$\ddot{\zeta} = \sigma \frac{\omega_c \, \omega}{c} \left( \dot{\xi} f(\xi, \eta, \zeta, \theta) + \dot{\eta} g(\xi, \eta, \zeta, \theta) \right), \tag{12c}$$

$$c\ddot{\theta} = \sigma \frac{\omega_c \omega}{c} \left( \dot{\xi} f(\xi, \eta, \zeta, \theta) + \dot{\eta} g(\xi, \eta, \zeta, \theta) \right),$$
 (12d)

where  $\xi(\tau), \eta(\tau), \zeta(\tau)$  are the space components and  $\theta(\tau)$  is the time component of the four-vector  $\xi^{\mu}(\tau)$ . To save space we dropped the dependence on  $\tau$ . The dots denote derivatives with respect to the proper time  $\tau$ . The two cyclotron frequencies  $\omega_c = eB/m$  and  $\omega_0 = eB_0/m$  measure the strength of the wave and of the constant magnetic field, respectively. They can be either positive or negative. The negative value of  $\omega_0$  means the reversal of the magnetic field direction.

From now on, we shall assume that  $\sigma=1$  because the equations of motion (12) with the functions f and g defined by (10) are invariant under the following transformation

$$\sigma \to -\sigma, \quad \xi \longleftrightarrow \eta, \quad \omega_0 \to -\omega_0.$$
 (13)

Therefore, we do not obtain anything essentially new by considering both signs of  $\sigma$ , since to every trajectory for  $\sigma = -1$  there corresponds a trajectory for  $\sigma = 1$  in the reversed constant magnetic field, differing only by a reflection with respect to the x = y plane.

The Lorentz equations (12) are nonlinear but they can be effectively linearized owing to conservation laws. In doing so, we shall follow the procedure developed in Ref. [2]. The first constant of motion  $\mathcal{E}$  is obtained by subtracting Eq. (12c) from Eq. (12d) which gives  $\ddot{\theta} - \ddot{\zeta}/c = 0$  or  $\dot{\theta} - \dot{\zeta}/c = \mathrm{const}_1$ . Thus,  $\mathcal{E}$  is a conserved quantity

$$\mathcal{E} = \dot{\theta} - \dot{\zeta}/c = \sqrt{1 + (\dot{\xi}^2 + \dot{\eta}^2 + \dot{\zeta}^2)/c^2} - \dot{\zeta}/c.$$
 (14)

Apart from the factor  $mc^2$ , the constant  $\mathcal{E}$  is the light-front energy — the conjugate variable to  $t_+ = t + z/c$ 

$$\mathcal{E} = \frac{1 - v_z/c}{\sqrt{1 - v^2/c^2}} = \frac{\sqrt{m^2c^4 + p^2c^2} - p_zc}{mc^2}.$$
 (15)

We shall assume that we start counting the proper time  $\tau$  in such a way that  $\theta(0) - \zeta(0)/c = 0$ . Under this assumption, Eq. (14) integrated with respect to  $\tau$  yields

$$\theta - \zeta/c = \mathcal{E}\,\tau. \tag{16}$$

Hence, the proper time is simply proportional to the light-front variable and this will enable us to separate the transverse motion from the longitudinal motion.

The second constant of motion is obtained by subtracting from Eq. (12c) the sum of Eq. (12a) multiplied by  $\dot{\xi}/\mathcal{E}$  and Eq. (12b) multiplied by  $\dot{\eta}/\mathcal{E}$ . Since the right hand sides cancel, we obtain

$$\dot{\zeta} - \frac{1}{2c\mathcal{E}}(\dot{\xi}^2 + \dot{\eta}^2) = \text{const}_2 = \frac{c}{2}(\frac{1}{\mathcal{E}} - \mathcal{E}). \tag{17}$$

The last expression is obtained by rearranging the formula  $1 + (\xi^2 + \dot{\eta}^2 + \dot{\zeta}^2)/c^2 = (\mathcal{E} + \dot{\zeta}/c)^2$  obtained from Eq. (14).

Owing to Eq. (14), the longitudinal motion affects the transverse motion only through the value of  $\mathcal E$  and since it is a constant of motion the equations for  $\xi$  and  $\eta$  may be solved first. The integration of Eqs. (12a-12b) is made simpler by introducing a complex combination of the coordinates  $Z=\xi+i\eta$ . The equation of motion for Z obtained from Eqs. (12) reads

$$\ddot{Z} = \omega_c \Omega Z^* e^{i\Omega \tau} - i\omega_0 \dot{Z}, \tag{18}$$

where in addition to the two cyclotron frequencies  $\omega_c$  and  $\omega_0$  associated with the strength of the wave and the constant magnetic field we defined the third frequency  $\Omega$  — an effective wave frequency as seen by the moving particle. Thus, the dynamics of the particle is governed by the three frequencies

$$\Omega = \omega \mathcal{E}, \quad \omega_c = \frac{eB}{m}, \quad \omega_0 = \frac{eB_0}{m}.$$
 (19)

The form  $\ddot{Z}e^{-i\Omega\tau/2}=\omega_c\Omega(Ze^{-i\Omega\tau/2})^*-i\omega_0\dot{Z}e^{-i\Omega\tau/2}$  of Eq. (18) suggests a transformation to the frame rotating (in proper time) with the angular velocity  $\Omega/2$  around the z-axis. This amounts to replacing  $\xi$  and  $\eta$  by the new variables

$$\alpha(\tau) = \xi(\tau)\cos(\Omega\tau/2) + \eta(\tau)\sin(\Omega\tau/2), \tag{20a}$$

$$\beta(\tau) = -\xi(\tau)\sin(\Omega\tau/2) + \eta(\tau)\cos(\Omega\tau/2), \qquad (20b)$$

or in complex notation

$$Z = \xi + i\eta = (\alpha + i\beta)e^{i\Omega\tau/2}.$$
 (21)

Upon substituting this expression into Eq. (18), we get rid of an explicit  $\tau$  dependence and obtain the following equations with constant coefficients for  $\alpha$  and  $\beta$ 

$$\ddot{\alpha} = (\Omega^2/4 + \Omega\omega_0/2 + \Omega\omega_c)\alpha + (\Omega + \omega_0)\dot{\beta}, \qquad (22a)$$

$$\ddot{\beta} = (\Omega^2/4 + \Omega\omega_0/2 - \Omega\omega_c)\beta - (\Omega + \omega_0)\dot{\alpha}.$$
 (22b)

The mutual relationships between the three frequencies  $\Omega$ ,  $\omega_c$ , and  $\omega_0$  determine whether the transverse motion is localized near the z axis or is unbounded.

A full description is most easily done in the Hamiltonian formalism. The equations of motion (22) can be obtained from the following Hamiltonian

$$H = \frac{p_{\alpha}^{2} + p_{\beta}^{2}}{2m} + m \frac{(a-b)\alpha^{2} + (a+b)\beta^{2}}{2} - w(\alpha p_{\beta} - \beta p_{\alpha}), \tag{23}$$

where

$$a = \frac{\omega_0^2}{4}, \quad b = \Omega \omega_c, \quad w = \frac{\Omega + \omega_0}{2}. \tag{24}$$

This Hamiltonian (for  $\omega_0 = 0$ ) differs by a canonical transformation from the one considered in Ref. [2]. We found this new form of the Hamiltonian more convenient than the previous one. The canonical equations of motion can be written in the following matrix form

$$i\frac{d}{dt}X = X \cdot \hat{M},\tag{25}$$

where

$$X = (\alpha, \beta, p_{\alpha}, p_{\beta}), \qquad (26)$$

and

$$\hat{M} = \begin{pmatrix} 0 & -iw & -im(a-b) & 0\\ iw & 0 & 0 & -im(a+b)\\ i/m & 0 & 0 & -iw\\ 0 & i/m & iw & 0 \end{pmatrix}. \quad (27)$$

We have absorbed i into the definition of the matrix M to make its eigenvalues equal to the (real) characteristic frequencies. These are the same equations of motion (only with different values of the coefficients) that govern the dynamics of particles in the mechanical model of the Paul trap [13, 14], Trojan asteroids in the Sun-Jupiter system and Trojan wave packets of Rydberg electrons in an electromagnetic wave [15] or in a molecule with an electric dipole moment [16]. As a matter of fact, every quadratic Hamiltonian, by an appropriate linear canonical transformation, can be reduced to the form (23).

The characteristic frequencies in the present case are

$$\Omega_{\pm} = \Omega r_{\pm}$$

$$r_{\pm} = \frac{1}{2} \sqrt{(1+\mu)^2 + \mu^2 \pm 4\sqrt{\nu^2 + \mu^2(1+\mu)^2/4}} , \quad (28)$$

where we used  $\Omega$  as a yard stick to measure all frequencies, i.e.

$$\mu = \omega_0 / \Omega, \quad \nu = \omega_c / \Omega.$$
 (29)

The description of the motion with the use of two dimensionless parameters  $\mu$  and  $\nu$  is very convenient because it exhibits a self-similarity inherent in our problem. The dimensionless ratios  $\mu$  and  $\nu$  provide a unified description of different physical situations. For example, a particle in a 2.45 GHz microwave oven will show the same behavior as a particle in an optical wave of a 505 nm blue laser provided we increase the amplitude of the wave and the strength of the magnetic field by a factor of  $2.42 \cdot 10^5$ . An increase/decrease of all three frequencies by the same factor does not change the character of the motion but it results in a decrease/increase of characteristic space and time scales. We shall take this fact into account and express the distances in the units of the angular wavelength  $\lambda = c/\omega$  and the time in the units of an angular period  $1/\omega$ . These units of length and time are used in all figures in this paper. In other words, we shall use units in which  $\omega = 1$  and c = 1.

Bounded oscillations occur only when both characteristic frequencies  $\Omega_{\pm}$  are real and this means that

$$|\nu| < \frac{1}{2} \left| \frac{1}{2} + \mu \right|.$$
 (30)

The mode amplitudes  $a_{\pm}$  and  $a_{\pm}^{*}$  (classical counterparts of the annihilation and creation operators) are found by solving the eigenvalue problem for the matrix  $\hat{M}$  appearing in Eq. (25)

$$a_{+} = \frac{1}{N_{+}^{1/2}} \left[ t_{++} \left( p_{\beta} - \frac{m\Omega s_{-}}{1+\mu} \alpha \right) - i\varepsilon t_{+-} \left( p_{\alpha} + \frac{m\Omega s_{+}}{1+\mu} \beta \right) \right], \qquad (31a)$$

$$a_{-} = \frac{1}{N_{-}^{1/2}} \left[ t_{--} \left( p_{\beta} + \frac{m\Omega s_{+}}{1+\mu} \alpha \right) + i\varepsilon t_{-+} \left( p_{\alpha} - \frac{m\Omega s_{-}}{1+\mu} \beta \right) \right], \qquad (31b)$$

where to save space we introduced the following functions of  $\mu$  and  $\nu$ 

$$s_{\pm} = \sqrt{\nu^2 + \mu^2 (1 + \mu)^2 / 4} \pm \nu,$$
 (32a)

$$t_{+\pm} = \sqrt{(1+\mu)^2 + 2s_{\pm}},$$
 (32b)

$$t_{-\pm} = \sqrt{|(1+\mu)^2 - 2s_{\pm}|},$$
 (32c)

$$\varepsilon = \operatorname{sign}(1 + \mu), \tag{32d}$$

and the normalization factors are

$$N_{+} = 4m\Omega_{+}(s_{+} + s_{-}). \tag{33}$$

This normalization guarantees that  $a_{\pm}$  and  $a_{\pm}^{*}$  have the canonical Poisson brackets

$$\{a_{\pm}, a_{+}^{*}\} = -i. \tag{34}$$

The formulas (31) are not valid when  $\mu = -1$ . However, in this special case the equations of motion (22) describe just two uncoupled harmonic oscillators and the determination of eigenmodes is very simple. The Hamiltonian (23) expressed through the amplitudes  $a_{\pm}$  reads

$$H = \Omega_{+} a_{+}^{*} a_{+} - \operatorname{sign}(1/2 + \mu) \Omega_{-} a_{-}^{*} a_{-}.$$
 (35)

The minus sign in the diagonal form of the Hamiltonian, indicates that for  $1/2 + \mu > 0$  the oscillations in the transverse plane are bounded due to the Coriolis force — a characteristic feature of the Paul trap or Trojan asteroids and Trojan electrons. We would like to stress that despite its quadratic form the Hamiltonian of the transverse motion does not correspond to a simple harmonic oscillator in two dimensions because the frequencies of oscillations  $\Omega_{\pm}$  are not fixed once and for all but they depend on the initial velocities through the parameter  $\mathcal{E}$ . The regions of stable motion in the  $\mu\nu$  plane are shown in Fig. 2.

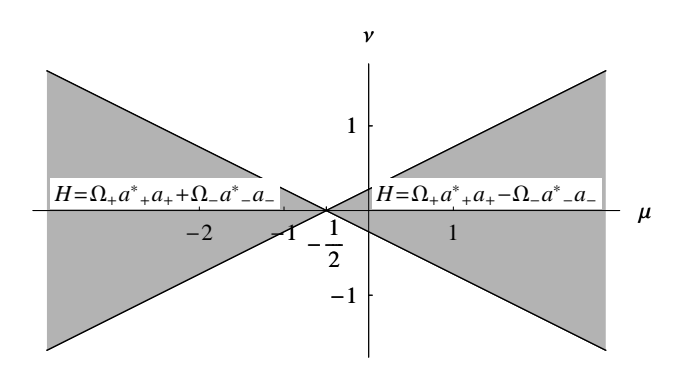


FIG. 2: Regions of stability in the  $\mu\nu$  plane are shown as two shaded areas. In the left area we have a normal harmonic oscillator while in the right area we have the Trojan regime — stable oscillations but the Hamiltonian is not positive definite.

The general solution for  $\xi(\tau)$  and  $\eta(\tau)$  in the laboratory frame is obtained by solving Eqs. (22) in terms of

eigenmodes and then undoing the rotation (20). The final expression for the motion of particles in the plane perpendicular to the vortex line can be compactly written in the same complex form as in [2]

$$\xi(\tau) + i\eta(\tau) = e^{i\Omega\tau/2} \left( (iD\kappa_+ + A)\sin(\Omega_+\tau) - (B\kappa_- + iC)\sin(\Omega_-\tau) + (iA\kappa_+ - D)\cos(\Omega_+\tau) + (C\kappa_- - iB)\cos(\Omega_-\tau) \right), \quad (36)$$

but the meaning of A, B, C, D, and  $\kappa_{\pm}$  is now different, namely

$$\kappa_{\pm} = \frac{r_{\pm}^2 + 1/4 + \mu/2 \pm \nu}{(1+\mu)r_{\pm}},\tag{37}$$

and the constants A, B, C, D are the following functions of the initial values of the transverse positions and velocities

$$A = \frac{(1/2 - \kappa_{-}r_{-})\eta_{0} + \dot{\xi}_{0}/\Omega}{r_{+} - r_{-}\kappa_{-}\kappa_{+}},$$
 (38a)

$$B = \frac{(\kappa_{+}/2 - r_{+})\eta_{0} + \kappa_{+}\dot{\xi}_{0}/\Omega}{r_{+} - r_{-}\kappa_{-}\kappa_{+}},$$
 (38b)

$$C = \frac{(1/2 - \kappa_{+} r_{+})\xi_{0} - \dot{\eta}_{0}/\Omega}{r_{-} - r_{+} \kappa_{-} \kappa_{+}},$$
 (38c)

$$D = \frac{(\kappa_{-}/2 - r_{-})\xi_{0} - \kappa_{-}\dot{\eta}_{0}/\Omega}{r_{-} - r_{+}\kappa_{-}\kappa_{+}}.$$
 (38d)

Having found the solution in the transverse plane, we can now just integrate Eq. (17) to obtain the following formula for the longitudinal motion

$$\zeta(\tau) = \frac{c\tau}{2} (\frac{1}{\mathcal{E}} - \mathcal{E}) + \int_0^{\tau} d\tau \frac{1}{2c\mathcal{E}} (\dot{\xi}^2 + \dot{\eta}^2) + \zeta(0). \quad (39)$$

The integration is cumbersome but elementary and it leads to

$$\zeta(\tau) = \frac{c\tau}{2} \left[ \frac{1}{\mathcal{E}} - \mathcal{E} + \frac{(A^2 + D^2) \left( (\Omega^2 + 4\Omega_+^2)(1 + \kappa_+^2) - 8\Omega\Omega_+ \kappa_+ \right) + (B^2 + C^2) \left( (\Omega^2 + 4\Omega_-^2)(1 + \kappa_-^2) - 8\Omega\Omega_- \kappa_- \right)}{8c^2 \mathcal{E}} \right]$$

$$+ \frac{(1 - \kappa_+^2)(\Omega^2 - 4\Omega_+^2) \left[ (D^2 - A^2) \sin(2\Omega_+ \tau) - 2AD(1 - \cos(2\Omega_+ \tau)) \right]}{32c \mathcal{E}\Omega_+}$$

$$+ \frac{(1 - \kappa_-^2)(\Omega^2 - 4\Omega_-^2) \left[ (B^2 - C^2) \sin(2\Omega_- \tau) + 2BC(1 - \cos(2\Omega_- \tau)) \right]}{32c \mathcal{E}\Omega_-}$$

$$+ \frac{(\kappa_+ - \kappa_-)(\Omega^2 - 4\Omega_+ \Omega_-) + 2(\kappa_+ \kappa_- - 1)\Omega\Omega_m}{8c \mathcal{E}\Omega_p} \left[ (CD - AB) \sin(\Omega_p \tau) - (AC + BD)(1 - \cos(\Omega_p \tau)) \right]$$

$$- \frac{(\kappa_+ + \kappa_-)(\Omega^2 + 4\Omega_+ \Omega_-) - 2(\kappa_+ \kappa_- + 1)\Omega\Omega_p}{8c \mathcal{E}\Omega_m} \left[ (CD + AB) \sin(\Omega_m \tau) - (AC - BD)(1 - \cos(\Omega_m \tau)) \right] + \zeta(0),$$

$$(40)$$

where  $\Omega_p = \Omega_+ + \Omega_-$  and  $\Omega_m = \Omega_+ - \Omega_-$ . Thus, the motion in the z direction is a composition of a uniform

motion in the proper time  $\tau$  (not in the laboratory time t) and oscillations with four frequencies  $2\Omega_{\pm}$  and  $\Omega_{+}\pm\Omega_{-}$ . By a fine tuning of the initial conditions we may cancel the uniform motion completely and leave only the oscillations, but any departure from these special values will cause a uniform drift. The appearance of two additional frequencies  $\Omega_{+}\pm\Omega_{-}$  is a new feature that is not found in the absence of the constant magnetic field. Note that the motion in the transverse plane is not completely decoupled from the longitudinal motion because the effective frequency  $\Omega$ , appearing abundantly in the formulas (36), depends (through  $\mathcal{E}$ ) on the initial velocity in the longitudinal direction.

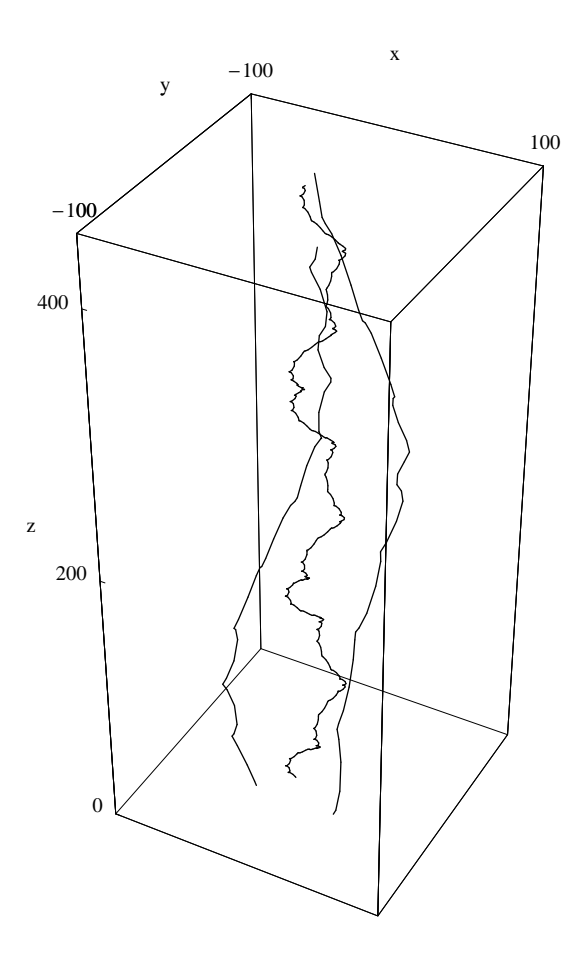


FIG. 3: Three trajectories obtained for  $\mu=0.075,\ \nu=0.1,$  and v/c=(0.001,0,0), differing only in the initial positions.

The presence of stability and instability windows is a manifestation of the *parametric resonance*. In the region of instability the amplitude of oscillations grows exponentially. This is essentially different as compared to the motion of a charged particle in the circularly polarized plane wave and a constant magnetic field. In that case there appears a standard resonance, i.e. the amplitude grows linearly when the frequency of the driving force (the wave) exactly matches the characteristic frequency

of the system (cyclotron frequency). When the circularly polarized wave is replaced by a wave with a vortex, the set of linear inhomogeneous differential equations becomes a set of homogeneous equations with periodically varying coefficients. The driving force disappears but the coefficients of the equation become now time dependent and there appears a parametric resonance. Its characteristic features are: the appearance of the whole regions of instability (and not only discrete values as in the case of an ordinary resonance) which shrink to just one point  $(\omega_0=-\omega/2)$  when  $\omega_c\to 0$  and an exponential growth of the amplitude in all regions of instability.

Three typical stable three-dimensional relativistic trajectories differing by the choice of initial positions are shown in Fig. 3. The trajectories of a particle projected on the xy plane for different values of the parameters  $\mu$  and  $\nu$  are shown in Figs. 4–6. The plots demonstrate that the characteristic shapes of the trajectories are very sensitive to the changes of these parameters.

#### B. Nonrelativistic limit

The solutions of the equations of motion in the nonrelativistic regime can be obtained from the relativistic ones just by formally taking the limit  $c \to \infty$ . In this limit, the difference between the proper time and the laboratory time disappears. Also, the wave frequency  $\omega$  and the effective frequency  $\Omega$  become equal, because  $\mathcal{E}=1$ . The motion in the longitudinal direction completely decouples from the oscillations in the transverse plane. In the nonrelativistic limit  $c(1/\mathcal{E}-\mathcal{E})/2 \to v_z$ . In this limit, the motion in the z direction becomes a free motion described by the formula  $z(t)=z_0+v_zt$ . In contrast to the relativistic case, the initial velocity in the z direction does not show any oscillations,  $v_z=v_{z0}$ . We arrive at the same conclusions by solving the nonrelativistic equations of motion  $(\sigma=1)$ 

$$\frac{d^2\xi}{dt^2} = \omega_c \,\omega \,(\xi \cos \omega t + \eta \sin \omega t) + \omega_0 \frac{d\eta}{dt},\tag{41a}$$

$$\frac{d^2\eta}{dt^2} = \omega_c \,\omega \,(\xi \sin \omega t - \eta \cos \omega t) - \omega_0 \frac{d\xi}{dt},\tag{41b}$$

$$\frac{d^2\zeta}{dt^2} = 0, (41c)$$

which are obtained from the Lorentz equations (12) in the limit  $c \to \infty$ . Since the decoupling of the longitudinal and the transverse motion in the nonrelativistic limit is complete, we may easily obtain in this case also the solutions for a two-dimensional gas of mutually noninteracting charged particles kept near the surface by an additional confining potential V(z).

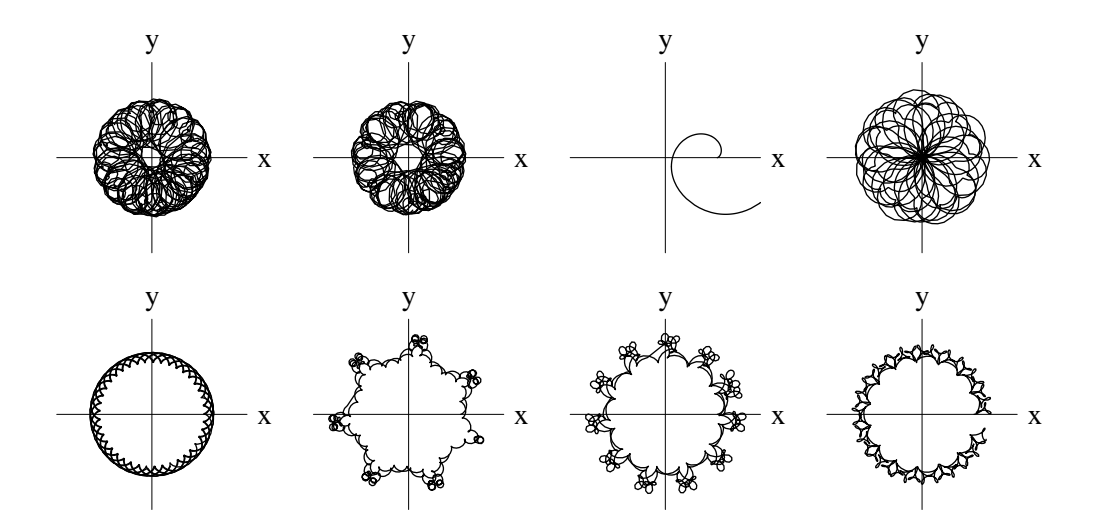


FIG. 4: The trajectories of a particle projected on the xy plane are shown for different values of the parameter  $\mu$  (i.e. for different values of the constant magnetic field)  $\mu = (-0.75, -0.7, -0.5, -0.2, 0.0, 0.1, 0.2, 0.4)$ . The value of  $\nu$  has been fixed at  $\nu = 0.075$ . The initial values of the position vectors (measured in  $\lambda = c/\omega$ ) and velocity vectors (measured in c) are (60, 0, 0) and (0.001, 0, 0.001), respectively. The size of the area shown in these plots is  $100\lambda \times 100\lambda$  and the time lapse is  $600/\omega$ . The third plot shows the exponential growth of the distance from the vortex line characteristic of the unstable regime.

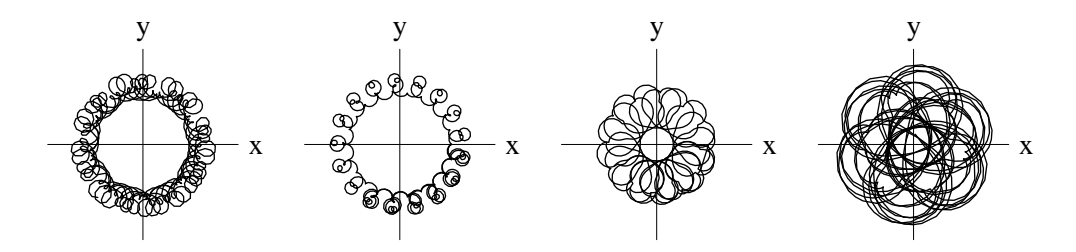


FIG. 5: The trajectories of a particle obtained for the same initial conditions as in Fig. 4. In these plots the value of  $\mu$  is fixed at  $\mu = -0.2$  but the strength of the field amplitude varies as follows  $\nu = (-0.1, -0.05, 0.05, 0.1)$ .

# IV. TRANSPORT OF ORBITS BY MOVING VORTICES

Orbits trapped by vortices can be moved around across the magnetic field. The simplest case is a uniform motion. The electromagnetic field with a moving vortex line can be easily obtained from the field with a stationary vortex line (9) by a Lorentz transformation. Assuming that the motion is along the x axis with velocity v, we obtain the following transformed electric and magnetic field vectors

$$\frac{\mathbf{E}_{v}}{B\omega} = \begin{pmatrix} \gamma(x - vt)\cos\varphi + y\sin\varphi \\ \gamma^{2}(x - vt)\sin\varphi - \gamma y\cos\varphi \\ -v(\gamma^{2}(x - vt)\cos\varphi + \gamma y\sin\varphi)/c \end{pmatrix}, \quad (42a)$$

$$\frac{cB_v}{B\omega} = \begin{pmatrix} -\gamma(x - vt)\sin\varphi + y\cos\varphi \\ \gamma^2(x - vt)\cos\varphi + \gamma y\sin\varphi \\ v(\gamma^2(x - vt)\sin\varphi - \gamma y\cos\varphi)/c \end{pmatrix}, (42b)$$

where  $\gamma = 1/\sqrt{1 - v^2/c^2}$  and  $\varphi = \omega(\gamma(t - vx/c^2) - z/c)$ . In Fig. 7 we show the trajectory of a particle that is being pulled across the constant magnetic field by the uni-

formly moving vortex line. Note, that this is not the same as transforming the whole problem to a moving frame by a Lorentz transformation. Such a transformation would result also in a change of the constant magnetic field into a crossed magnetic and electric fields.

The transport with a uniform average velocity is just the simplest example, but there is a plethora of more intricate cases — all of them exhibiting the same behavior. The simplest method to construct a solution of the Maxwell equations with a vortex line undergoing complicated motions is to superimpose our basic solution (9) with circularly polarized plane waves moving in the same direction, slightly detuned from the frequency  $\omega$ . We shall consider here two cases: a superposition with just one plane wave and a superposition with two waves. In the first case, the vortex position at a fixed value of z will move on a circle and in the second case it will follow a trefoil figure.

In the circular case, we shall chose the Riemann-

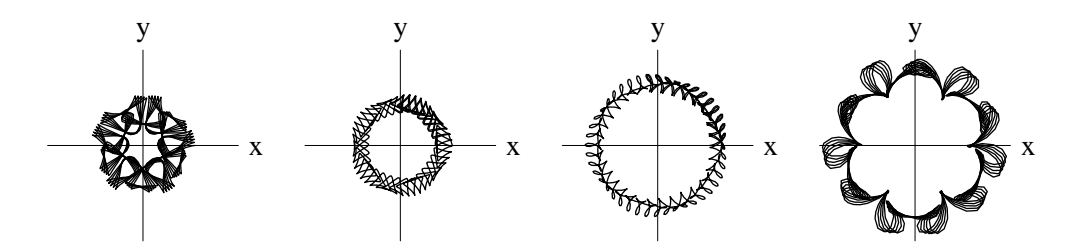


FIG. 6: The trajectories of a particle obtained for the same initial conditions as in Fig. 4. In these plots the value of  $\mu$  is fixed at  $\mu = 0.5$  but the strength of the field amplitude varies as follows  $\nu = (-0.2, -0.1, 0.1, 0.2)$ .

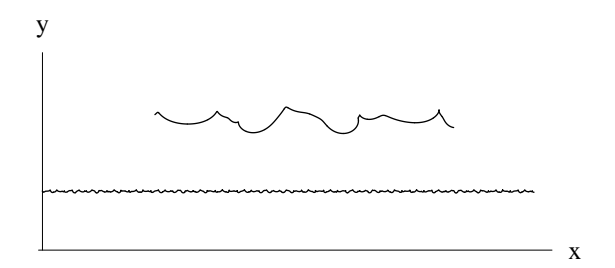
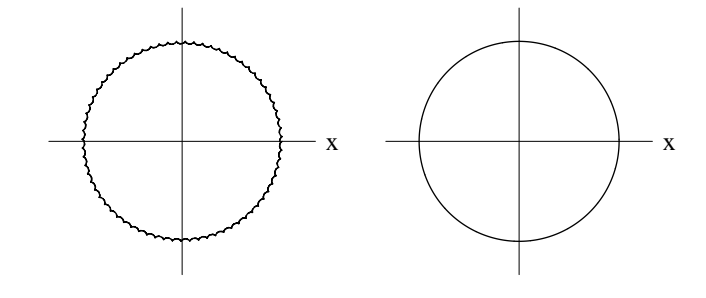


FIG. 7: The transport of an orbit by a moving vortex line. On top of the average motion with a constant velocity in the x direction we have additional oscillations, clearly seen in the upper part of the figure after a tenfold enlargement.



Silberstein vector in the form

$$\mathbf{F}_{c}(\mathbf{r},t) = B\omega \left(\hat{\mathbf{x}} + i\hat{\mathbf{y}}\right)$$

$$\times \left( (x+iy)e^{-i\omega(t-z/c)} - (x_1 + iy_1)e^{-i\omega_1(t-z/c)} \right), \quad (43)$$

where  $x_1$  and  $y_1$  are two parameters that fix the radius of the circle and the initial position of the vortex. The vanishing of the RS vector determines the position  $(x_v, y_v)$  of the vortex line as a function of z and t

$$x_v(z,t) + iy_v(z,t) = (x_1 + iy_1)e^{i(\omega - \omega_1)(t - z/c)}.$$
 (44)

The formulas for the electric and magnetic field vectors

$$\frac{\boldsymbol{E}_c}{B\omega} = \begin{pmatrix} x\cos\vartheta + y\sin\vartheta - x_1\cos\vartheta_1 - y_1\sin\vartheta_1\\ x\sin\vartheta - y\cos\vartheta - x_1\sin\vartheta_1 + y_1\cos\vartheta_1\\ 0 \end{pmatrix}, (45a)$$

$$\frac{c\mathbf{B}_c}{B\omega} = \begin{pmatrix} y\cos\vartheta - x\sin\vartheta - y_1\cos\vartheta_1 + x_1\sin\vartheta_1\\ y\sin\vartheta + x\cos\vartheta - y_1\sin\vartheta_1 - x_1\cos\vartheta_1\\ 0 \end{pmatrix}, (45b)$$

where  $\vartheta = \omega(t - z/c)$  and  $\vartheta_1 = \omega_1(t - z/c)$ . Thus, the vortex line forms a helix rotating with the angular frequency  $\omega - \omega_1$ . The projection of this helix on the xy plane forms a circle. In Fig. 8 we show the motion of the particle dragged by such a helical vortex line.

In order to obtain a more elaborate path (a generalized Lissajou figure) of the vortex in the xy plane, we add two

FIG. 8: The transport of an orbit by a vortex line moving on a circle. The projection of the trajectory on the xy plane (left) is to be compared with the path of the vortex line (right). The period of the circular motion was chosen as 2000 times the period T of the carrier wave and the time lapse for the trajectory shown in this figure is equal to the full period of the circular motion. The remaining parameters are  $\mu=0.1$  and  $\nu=0.07$ . The distances are measured in units of the wavelength  $\lambda=c/\omega$  of the carrier wave. The radius of the circle is 15  $\lambda$ . Initially the particle was placed at the position of the vortex ( $\xi_0=15,\ \eta_0=0$ ) with zero velocity.

plane waves, instead of one, i.e.

$$\mathbf{F}_{g}(\mathbf{r},t) = B\omega \left(\hat{\mathbf{x}} + i\hat{\mathbf{y}}\right) \left( (x+iy)e^{-i\omega(t-z/c)} - (x_1 + iy_1)e^{-i\omega_1(t-z/c)} - (x_2 + iy_2)e^{-i\omega_2(t-z/c)} \right).$$
(46)

In this case, the position of the vortex as a function of t and z is given by the equation

$$x_v(z,t) + iy_v(z,t) = (x_1 + iy_1)e^{i(\omega - \omega_1)(t - z/c)}$$

$$(x_2 + iy_2)e^{i(\omega - \omega_2)(t - z/c)}.$$
 (47)

The numerical solutions presented here in Figs. 4–10 should leave no doubt that an electromagnetic vortex may easily overcome the inertia of the particle and drag the cyclotron orbit along. Analytic solutions of the equations of motion for a particle in the presence of electromagnetic waves with moving vortices can also be obtained and they will be described elsewhere.

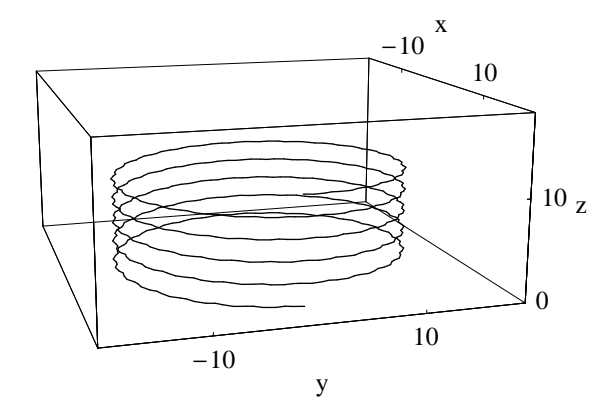


FIG. 9: The same trajectory as in Fig. 8 plotted in three dimensions for five periods of the circular motion.

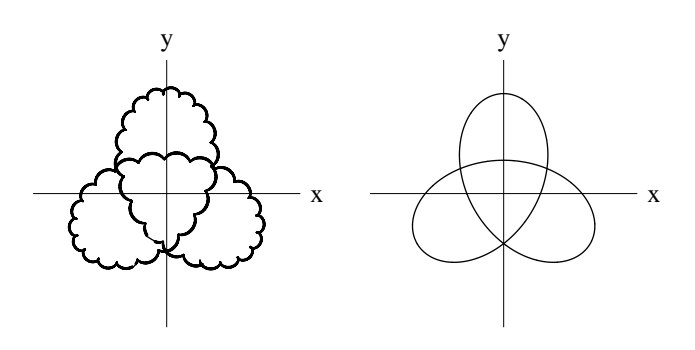


FIG. 10: The transport of an orbit by a vortex line moving along a trefoil. The two frequencies in the formula (46) are  $1.0005\,\omega$  and  $0.999\,\omega$ . Since the two detunings are commensurate, the trajectory (right) of the vortex line in the xy plane is closed. The parameters characterizing the position of the vortex are  $x_1=5,\,y_1=0,\,x_2=0,\,y_2=-10$ . The remaining parameters are  $\mu=10$  and  $\nu=1.5$ . The distances are measured in units of the wavelength  $\lambda=c/\omega$  of the carrier wave. Initially the particle is placed on the vortex line at  $\xi_0=5$  and  $\eta_0=-10$  with zero velocity. The size of the area in these figures is  $20\lambda\times20\lambda$ .

#### V. QUANTUM MECHANICS

We shall first describe the motion of a quantum particle in the combination of an electromagnetic wave with a vortex line (9) and a constant magnetic field in a fully relativistic case. The nonrelativistic limit will be obtained by a simple reinterpretation of the parameters. Also, the incorporation of spin does not introduce any significant complications. Therefore, we shall start with the Dirac equation.

#### A. Relativistic quantum mechanics

The Dirac equation for a particle moving in the presence of an electromagnetic field described by a vector potential  $\boldsymbol{A}(\boldsymbol{r},t)$  can be written in the form

$$i\hbar\partial_t\Psi = (c\boldsymbol{\alpha}\cdot(-i\hbar\boldsymbol{\nabla} - e\boldsymbol{A}) + \beta mc^2)\Psi.$$
 (48)

In our case, the vector potential can be chosen as

$$\mathbf{A}(\mathbf{r},t) = \begin{pmatrix} -Bg(\mathbf{r},t) - yB_0/2 \\ Bf(\mathbf{r},t) + xB_0/2 \\ 0 \end{pmatrix}. \tag{49}$$

The quantum counterpart of the classical symmetry transformation (13), namely

$$\sigma \to -\sigma, \ x \longleftrightarrow y, \ \omega_0 \to -\omega_0, \ \Psi \to \frac{1 + \alpha_x \alpha_y}{\sqrt{2}} \Psi, \ (50)$$

leaves the Dirac equation invariant. Therefore, we may again restrict ourselves to the case  $\sigma=1$  and obtain the solution for  $\sigma=-1$  by applying the transformation (50). It is convenient to choose the Dirac representation [17] of  $\alpha_i$  and  $\beta$  but with the matrices  $\alpha_z$  and  $\beta$  interchanged, i.e.

$$\alpha_x = \rho_x \sigma_x, \ \alpha_y = \rho_x \sigma_y, \ \alpha_z = \rho_z, \ \beta = \rho_x \sigma_z,$$
 (51)

where  $\rho_i$  and  $\sigma_i$  are two sets of Pauli matrices acting independently. Next, we split the four component bispinor into two-component wave functions with the help of two projection operators  $P_{\pm} = (1 \pm \alpha_z)/2$ . In the representation (51), the matrix  $\alpha_z$  is diagonal and the splitting amounts to taking the upper and lower components of the Dirac bispinor  $\Psi$ . Therefore, we may write

$$\Psi = P_{+}\Psi + P_{-}\Psi = \begin{pmatrix} \Psi_{+} \\ 0 \end{pmatrix} + \begin{pmatrix} 0 \\ \Psi_{-} \end{pmatrix}$$
 (52)

and the Dirac equation (48) takes on the form

$$2i\hbar\partial_{+}\Psi_{+} = \hat{h}\,\Psi_{-},\tag{53a}$$

$$2i\hbar\partial_{-}\Psi_{-} = \hat{h}\,\Psi_{+},\tag{53b}$$

where  $\partial_{\pm} = \partial/\partial t_{\pm} = (\partial_t \pm c\partial_z)/2$  and

$$\hat{h} = c \left( mc\sigma_z - \boldsymbol{\sigma}_{\perp} \cdot (i\hbar \nabla + e\boldsymbol{A}) \right). \tag{54}$$

From now on, all capitalized Greek letters denote twocomponent spinor wave functions. In the next step, following the procedure of Ref. [2], we perform the transformation to the rotating frame to eliminate the dependence of the potential on t-z/c. To this end, we make the following substitutions in Eqs. (53)

$$\Psi_{\pm} = U\tilde{\Psi}_{\pm} = e^{-i\frac{\omega t_{-}}{2\hbar}\hat{M}_{z}}\tilde{\Psi}_{\pm}, \tag{55}$$

where  $\hat{M}_z$  is the z component of the total angular momentum

$$\hat{M}_z = \hat{L}_z + \frac{\hbar}{2}\sigma_z = \frac{\hbar}{i}(x\partial_y - y\partial_x) + \frac{\hbar}{2}\sigma_z.$$
 (56)

Under the transformation (55), the z components of all vector operators,  $\mathbf{r}, \nabla$ , and  $\boldsymbol{\sigma}$  do not change while the x and y components undergo a rotation, for example,

$$U^{\dagger}xU = x\cos(\omega t_{-}/2) - y\sin(\omega t_{-}/2), \tag{57a}$$

$$U^{\dagger}yU = x\sin(\omega t_{-}/2) + y\cos(\omega t_{-}/2). \tag{57b}$$

Applying these transformations to both equations (53) we obtain

$$2i\hbar\partial_{+}\tilde{\Psi}_{+} = \hat{h}_{0}\tilde{\Psi}_{-}, \tag{58a}$$

$$(2i\hbar\partial_{-} + \omega \hat{M}_z)\tilde{\Psi}_{-} = \hat{h}_0\,\tilde{\Psi}_{+},\tag{58b}$$

where

$$\hat{h}_0 = c \left( mc\sigma_z - \boldsymbol{\sigma}_\perp \cdot (i\hbar \nabla + e\boldsymbol{A}_0) \right), \tag{59}$$

and  $\mathbf{A}_0$  is the vector potential (49) evaluated at  $t_- = 0$ ,

$$\mathbf{A}_0 = ((B - B_0/2)y, (B + B_0/2)x, 0). \tag{60}$$

Since now there is no explicit dependence on t and z, we may seek solutions of Eqs. (58) by separating these variables

$$\tilde{\Psi}_{\pm}(x, y, z, t) = e^{-i(Et - p_z z)/\hbar} \Phi_{\pm}(x, y), \tag{61}$$

where E and  $p_z$  are the separation constants. The equations for  $\tilde{\Psi}_{\pm}(x,y)$  have the form

$$(E - p_z c)\Phi_+ = \hat{h}_0 \Phi_-,$$
 (62a)

$$(E + p_z c + \omega \hat{M}_z)\Phi_- = \hat{h}_0 \Phi_+, \tag{62b}$$

and upon the elimination of  $\Phi_+$ , we obtain the following eigenvalue equation for the transverse motion

$$\left(\frac{(i\hbar\nabla + e\mathbf{A}_0)^2}{2m} - \frac{\hbar\omega_0}{2}\sigma_z - \frac{\Omega}{2}\hat{M}_z\right)\Phi_- = E_\perp\Phi_-, (63)$$

where the energy of the transverse motion is defined as

$$E_{\perp} = \frac{E^2 - m^2 c^4 - (p_z c)^2}{2mc^2} \tag{64}$$

and the effective frequency  $\Omega = \mathcal{E}\omega = (E - p_z c)\omega/mc^2$  is the same as in the classical theory (cf. Eq. (15)).

We shall now determine the eigenvalues and the eigenfunctions of the Hamiltonian appearing in (63). Upon the substitution of the explicit form (60) of the vector potential  $\mathbf{A}_0$ , we obtain the following equation

$$\left[ -\frac{\hbar^2}{2m} \Delta_{\perp} + \frac{m}{2} \left( \omega_c + \frac{\omega_0}{2} \right)^2 x^2 + \frac{m}{2} \left( \omega_c - \frac{\omega_0}{2} \right)^2 y^2 + i\hbar \omega_c (x\partial_y + y\partial_x) - \frac{\omega_0 + \Omega}{2} \hat{L}_z - \hbar \left( \frac{\omega_0}{2} + \frac{\Omega}{4} \right) \sigma_z \right] \Phi_- = E_{\perp} \Phi_-, \quad (65)$$

where  $\hat{L}_z$  is the z component of the orbital angular momentum. This equation, by a substitution

$$\Phi_{-} = e^{im\omega_c xy/\hbar} \Phi, \tag{66}$$

is transformed to the final form

$$\left[ -\frac{\hbar^2}{2m} \Delta_{\perp} + \frac{m}{2} \left( \frac{\omega_0^2}{4} - \omega_c \Omega \right) x^2 + \frac{m}{2} \left( \frac{\omega_0^2}{4} + \omega_c \Omega \right) y^2 - \frac{\omega_0 + \Omega}{2} \hat{L}_z - \hbar \left( \frac{\omega_0}{2} + \frac{\Omega}{4} \right) \sigma_z \right] \Phi = E_{\perp} \Phi.$$
(67)

The Hamiltonian in this equation differs only by the spin term from the classical Hamiltonian (23). Since the spin part contributes only an energy shift, we may use the classical amplitudes of normal modes (31) to construct the annihilation operators

$$\hat{a}_{+} = \frac{1}{(\hbar N_{+})^{1/2}} \left[ t_{++} \left( \frac{\hbar}{i} \partial_{y} - \frac{m\Omega s_{-}}{1+\mu} x \right) - i\varepsilon t_{+-} \left( \frac{\hbar}{i} \partial_{x} + \frac{m\Omega s_{+}}{1+\mu} y \right) \right], \qquad (68a)$$

$$\hat{a}_{-} = \frac{1}{(\hbar N_{-})^{1/2}} \left[ t_{--} \left( \frac{\hbar}{i} \partial_{y} + \frac{m\Omega s_{+}}{1+\mu} x \right) + i\varepsilon t_{-+} \left( \frac{\hbar}{i} \partial_{x} - \frac{m\Omega s_{-}}{1+\mu} y \right) \right]. \qquad (68b)$$

The normalization of these operators is different from their classical counterparts by a factor of  $1/\sqrt{\hbar}$  to secure the proper commutation relations. The quantum Hamiltonian, appearing in Eq. (67), expressed in terms of the creation and annihilation operators is (without the spin term)

$$\hat{H} = \hbar \Omega_{+} \hat{a}_{+}^{\dagger} \hat{a}_{+} - \text{sign}(1/2 + \mu) \hbar \Omega_{-} \hat{a}_{-}^{\dagger} \hat{a}_{-} + \frac{\hbar \Omega_{+}}{2} - \text{sign}(1/2 + \mu) \frac{\hbar \Omega_{-}}{2},$$
 (69)

where we have used the relations  $t_{\pm+}t_{\pm-}=2|1+\mu|\Omega_{\pm}$ . It differs from the classical expression (35) by the usual zero-point energy terms.

Now, we shall determine a Gaussian wave function annihilated by the operators  $\hat{a}_{\pm}$ . We may do so by substituting a Gaussian wave function in the form

$$\psi_0 = \exp(-q_x x^2/2 - q_y y^2/2 - iqxy) \tag{70}$$

into the equations

$$\hat{a}_{+}\psi_{0} = 0, \quad \hat{a}_{-}\psi_{0} = 0 \tag{71}$$

and find  $q_x, q_y$  and q. By comparing the coefficients at x and y in the equations (71), we obtain the following set of 4 linear equations for the three parameters  $q_x, q_y$  and q

$$q_{x}|1 + \mu| t_{+-} - q(1 + \mu) t_{++} = m\Omega s_{-}t_{++}/\hbar, \quad (72a)$$

$$q_{y}|1 + \mu| t_{++} + q(1 + \mu) t_{+-} = m\Omega s_{+}t_{+-}/\hbar, \quad (72b)$$

$$q_{x}|1 + \mu| t_{-+} + q(1 + \mu) t_{--} = m\Omega s_{+}t_{--}/\hbar, \quad (72c)$$

$$q_{y}|1 + \mu| t_{--} - q(1 + \mu) t_{-+} = m\Omega s_{-}t_{-+}/\hbar. \quad (72d)$$

There exists a solution of these equations and it reads

$$q_x = \varpi(s_+ + s_-)t_{++}t_{--},\tag{73a}$$

$$q_y = \varpi(s_+ + s_-)t_{+-}t_{-+},\tag{73b}$$

$$q = \varepsilon \varpi (s_{+}t_{+-}t_{--} - s_{-}t_{++}t_{-+}),$$
 (73c)

where

$$\varpi = \frac{m\Omega}{\hbar |1 + \mu|(t_{++} + t_{-+} + t_{+-} t_{--})}.$$
 (74)

The Gaussian wave function (70) describes an analog of the ground state of the system. This will not always be a true ground state because for  $\mu > -1/2$  the Hamiltonian is not positive definite. Having found the state  $\psi_0$  we may generate a complete set  $\psi_{mn}$  of "excited" states by acting on  $\psi_0$  with powers of the creation operators

$$\psi_{mn} = \hat{a}_{+}^{\dagger m} \hat{a}_{+}^{\dagger n} \psi_{0}. \tag{75}$$

The wave functions representing these states are Gaussians (70) multiplied by the polynomials in the variables x and y of the (m+n)-th order. All wave functions (75) are localized around the vortex line. A complete set of two-component wave functions can be obtained from the one-component functions  $\psi_{mn}$  by attaching two independent two-component spinors  $u_+$ 

$$\Phi_{mn+} = \psi_{mn} u_+. \tag{76}$$

Choosing the spinors  $u_{\pm}$  in the form  $u_{+} = (1,0)$  and  $u_{-} = (0,1)$  we obtain for each choice of m and n two solutions of the eigenvalue equation (67) of the same shape and differing only in the energy eigenvalues.

Having reduced the problem to a two-dimensional harmonic oscillator, we may use the whole arsenal of tools available in this case. We may combine the classical trajectories with the solutions of the wave equations and construct quantum counterparts of classical motions. Namely, with each pair made of a classical solution of the equations of motion described by the Hamiltonian (23) and a localized wave function (75) we may associate a new solution of the wave equation in the form of a displaced wave function [18, 19] representing a localized wave packet moving along the classical trajectory. These states correspond to coherent states of quantum optics. We may also introduce the analogs of optical squeezed states described by Gaussian wave functions whose shapes are changing during the time evolution.

We did not study numerical solutions of the Dirac equation in the presence of moving vortices but the close correspondence between the classical and quantum dynamics exhibited for a stationary vortex makes us believe that the transport of the orbits by moving vortices, seen in the classical case, must carry over to the quantum case.

#### B. Nonrelativistic limit

The eigenvalue equation (63) does not contain the speed of light. Therefore, one may suspect that it co-

incides with the energy eigenvalue problem for a nonrelativistic charged particle in a coordinate frame rotating with angular frequency  $\Omega/2$ . We may confirm this observation by neglecting the relativistic corrections from the very beginning. This amounts to using the nonrelativistic Schrödinger-Pauli equation instead of the Dirac equation

$$i\hbar\partial_t\Psi = \left(-\frac{\hbar^2}{2m}\left(\nabla - \frac{ie}{\hbar}\boldsymbol{A}_{nr}\right)^2 - \frac{e\hbar}{2m}\boldsymbol{\sigma}\cdot\boldsymbol{B}_0\right)\Psi, (77)$$

where in the spirit of the nonrelativistic approximation we have neglected retardation in the expression (49) for the vector potential

$$\mathbf{A}_{nr}(\mathbf{r},t) = \begin{pmatrix} B(y\cos\omega t - x\sin\omega t) - yB_0/2\\ B(x\cos\omega t + y\sin\omega t) + xB_0/2\\ 0 \end{pmatrix}. \quad (78)$$

Note that in the Schrödinger-Pauli equation the the magnetic moment is coupled only to  $B_0$  because the magnetic field generated by the vector potential (78) has only the constant part. After the transformation to the rotating frame we obtain the same eigenvalue equation as in (63). Thus, the solutions of the eigenvalue problem obtained in the full relativistic theory can be used, without any modifications, in the nonrelativistic case.

#### VI. SUMMARY

We have shown that classical (cyclotron) and quantum (Landau) orbits of a charged particle in a constant magnetic field can be controlled by electromagnetic waves with embedded vortex lines. These orbits are pinned down in the vicinity of the vortex line and are dragged along when the vortex line moves in the plane perpendicular to the magnetic field. We analyzed this behavior with the use of our new analytic solutions of the Lorentz equations of motion in the classical case and the Dirac (or Schrödinger) wave equation in the quantum case. We have shown that the trapping of orbits by the vortex in the classical case has its counterpart in the form of Gaussian shape of the wave functions localized in the vicinity of the vortex. The effective reduction of the dynamics of our system to that of a two-dimensional harmonic oscillator makes it possible to give a complete solution using many tools developed in the past for oscillators. In particular, with the use of creation operators we have constructed a complete set of states. Coherent states the closest analogs of classical orbits — are also easily constructed.

### Acknowledgments

We would like to thank Zofia Bialynicka-Birula and Tomasz Sowiński for useful comments. This research has been partly supported by the Grant 008/P03/2003.

- [1] C. S. Roberts and S. J. Buchsbaum, Motion of a charged particle in a constant magnetic field and a transverse electromagnetic wave propagating along the field, Phys. Rev. 135, A381 (1964).
- [2] I. Bialynicki-Birula, Particle Beams Guided by Electromagnetic Vortices: New Solutions of the Lorentz, Schrödinger, Klein-Gordon, and Dirac Equations, Phys.Rev. Lett. 93, 020402 (2004).
- [3] S. Wolfram, The Mathematica Book, 5th ed, Wolfram Media, 2003.
- [4] G. Y. Rainich, Electrodynamics in the general relativity theory, Trans. Am. Math. Soc. 27, 106 (1925).
- [5] I. Bialynicki-Birula and Z. Bialynicka-Birula, Vortex lines of the electromagnetic field, Phys. Rev. A 67, 062114 (2003).
- [6] I. Bialynicki-Birula, Electromagnetic vortices riding atop null solutions of the Maxwell equations, J. Opt. A: Pure Appl. Opt. 6 (2004) S181.
- [7] L. Allen, M. J. Padgett, and M. Babiker, The orbital angular momentum of light, Progress in Optics, Vol. 39, edited by E. Wolf, Elsevier, Amsterdam, 1999.
- [8] J. Stratton, Electromagnetic Theory, McGraw-Hill, New York, 1941, Ch. VI.
- [9] I. Bialynicki-Birula, Photon wave function in Progress in Optics, edited by E. Wolf Elsevier, Amsterdam, 1996; arXiv:/quant-ph/0508202.
- [10] E. T. Whittaker, On an expression of the electromagnetic field due to electrons by means of two scalar potential functions, Proc. Lond. Math. Soc. 1 (1904) 367.
- [11] I. Bialynicki-Birula and Z. Bialynicka-Birula, Beams

- of electromagnetic field carrying angular momentum: The Riemann-Silberstein vector and the classical-quantum correspondence, Opt. Comm. in print; xrXiv:/physics/0502025.
- [12] I. Bialynicki-Birula, Z. Bialynicka-Birula and B. Chmura, Trojan states of electrons guided by electromagnetic vortices, Laser Physics 15, 1371 (2005); arXiv: physics/0309112.
- [13] W. Paul, Electromagnetic traps for charged and neutral particles, Rev. Mod. Phys. 62, 531 (1990).
- [14] I. Bialynicki-Birula and T. Sowiński, Gravity-induced resonances in a rotating trap, Phys. Rev. A 71, 043610 (2005); arXiv:/quant-ph/0412004.
- [15] I. Bialynicki-Birula, M. Kalinski, and J. H. Eberly, Lagrange equilibrium points in celestial mechanics and non-spreading wave packets for strongly driven Rydberg electrons, Phys. Rev. Lett. 73, 1777 (1994).
- [16] I. Bialynicki-Birula and Z. Bialynicka-Birula, Nonspreading wave packets for Rydberg electrons in rotating molecules with electric dipole moments, Phys. Rev. Lett. 77, 4298 (1996).
- [17] P. A. M. Dirac, Principles of Quantum Mechanics, Oxford University Press, Oxford, 1958.
- [18] J. F. Dobson, Harmonic-potential theorem: Implications for approximate many-body theories, Phys. Rev. Lett. 73, 2244 (1994).
- [19] I. Bialynicki-Birula and Z. Bialynicka-Birula, Center-ofmass motion in the many-body theory of Bose-Einstein condensates, Phys. Rev. A 65, 63606 (2002).